JCS ePress online publication date 2 September 2003

Mutations in the motor domain modulate myosin activity and myofibril organization

Qun Wang[1], Carole L. Moncman[2] and Donald A. Winkelmann[1,*]

[1]Department of Pathology and Laboratory Medicine, Robert Wood Johnson Medical School, Piscataway, NJ 08854, USA
[2]Department of Molecular and Cellular Biochemistry, University of Kentucky, Lexington, KY 40536, USA
*Author for correspondence (e-mail: daw@pleiad.umdnj.edu)

Accepted 11 June 2003
Journal of Cell Science 116, 4227-4238 © 2003 The Company of Biologists Ltd
doi:10.1242/jcs.00709

Summary

We have investigated the functional impact on cardiac myofibril organization and myosin motor activity of point mutations associated with familial hypertrophic cardiomyopathies (FHC). Embryonic chicken cardiomyocytes were transfected with vectors encoding green fluorescent protein (GFP) fused to a striated muscle myosin heavy chain (GFP-myosin). Within 24 hours of transfection, the GFP-myosin is found co-assembled with the endogenous myosin in striated myofibrils. The wild-type GFP-myosin had no effect on the organization of the contractile cytoskeleton of the cardiomyocytes. However, expression of myosin with the R403Q FHC mutation resulted in a small but significant decrease in myofibril organization, and the R453C and G584R mutations caused a more dramatic increase in myofibril disarray. The embryonic cardiomyocytes beat spontaneously in culture and this was not affected by expression of the wild-type or mutant GFP-myosin. For the biochemical analysis of myosin motor activity, replication defective adenovirus was used to express the wild-type and mutant GFP-myosin in C2C12 myotubes. The R403Q mutation enhanced actin filament velocity but had no effect on the myosin duty ratio. The R453C and G584R mutations impaired actin filament movement and both increased the duty ratio. The effects of these mutations on myosin motor activity correlate with changes in myofibril organization of live cardiomyocytes. Thus, mutations associated with hypertrophic cardiomyopathies that alter myosin motor activity can also impair myofibril organization.

Movies available online

Key words: Myosin, Myofibril, Hypertrophic, Cardiomyopathy, GFP

Introduction

Mutations in the structural components of muscle are directly responsible for a class of human disease, familial hypertrophic cardiomyopathy (FHC) (Bonne et al., 1998; Seidman and Seidman, 2001; Watkins et al., 1995c). The disease is characterized by cardiac hypertrophy primarily affecting the left ventricle and the intraventricular septum that occurs in the absence of other known conditions leading to hypertrophy. The myocardium of affected individuals is often marked by foci of disorganized myocytes, cellular disarray affecting the organization of the contractile apparatus, myofibril disarray and increased fibrosis (Ferrans et al., 1972). The disease is associated with a high incidence of sudden cardiac arrest and death (Towbin, 2001).

The β-cardiac myosin heavy chain gene, the predominant myosin expressed in adult human hearts, was the first genetic locus associated with FHC (Geisterfer-Lowrance et al., 1990). It is now clear that FHC is genetically heterogeneous mapping to at least nine separate loci. Over 50 different FHC alleles have been identified in the β-cardiac myosin heavy chain gene, and alleles at this locus produce considerable clinical variation in pathophysiology (Seidman and Seidman, 2000). Over 75% are missense mutations within the myosin motor domain that cluster in four distinct functional regions: the ATP binding site, the actin binding interface, the reactive sulfhydryl or converter region and the light chain binding domain (Rayment et al., 1995). Alleles mapping to the essential and regulatory cardiac myosin light chains have also been reported (Poetter et al., 1996). Aside from the cardiac myosin subunits, six other genetic loci, all encoding proteins of the muscle sarcomere, have been linked to FHC, leading to the hypothesis that FHC is a disease of the sarcomere (Seidman and Seidman, 2001). These include: cardiac α-actin (Mogensen et al., 1999), α-tropomyosin (Laing et al., 1995; Thierfelder et al., 1994), cardiac troponin T and I (Kimura et al., 1997; Thierfelder et al., 1994; Watkins et al., 1995b), myosin binding protein C and titin (Bonne et al., 1995; Watkins et al., 1995a).

The effect of FHC mutations on myosin activity has been actively studied either by in vitro analysis of myosin motor activity (Cuda et al., 1997; Fujita et al., 1997; Miller et al., 2003; Palmiter et al., 2000; Sweeney et al., 1994; Tyska et al., 2000; Yamashita et al., 2000), or by the generation of animal models of the disease (Geisterfer-Lowrance et al., 1996; Maass and Leinwand, 2000; Marian et al., 1999). Reduced and enhanced myosin functional activity has been reported for some of the FHC mutants, but it remains unclear how the altered functional activity can lead to the morphological disarray observed in FHC hearts. While it is possible that myosin mutations associated with FHC disrupt myofibril assembly and lead directly to myofibril disarray, it is also possible that the disarray is a secondary effect of changes in global cardiac function and loading.

Here we describe an approach for following the expression

and assembly of striated muscle myosin in living embryonic chicken cardiomyocytes. A chimeric striated muscle myosin was created by fusing green fluorescent protein (GFP) to the myosin N terminus (GFP-myosin). The GFP-myosin participates fully in the muscle specific cytoskeleton of live embryonic cardiomyocytes and contributes to the establishment of the contractile phenotype of these cells. This approach has been used to analyze the effect of FHC point mutations in the motor domain on the organization and activity of the contractile cytoskeleton in these cells. We demonstrate myofibril disarray in cells transfected with GFP-myosin carrying specific FHC mutations. The motor activity of wild-type (WT) and mutant GFP-myosin was analyzed after expression of these proteins in myotubes. The FHC mutations caused changes in the myosin motor activity and the myosin duty ratio that mirror the effects of these mutations on the myofibril organization of cardiomyocytes. Thus, FHC mutations that affect myosin motor activity can disrupt myofibril organization in a manner that is characteristic of this disease in the absence of other contributing factors.

Materials and Methods

Construction of a GFP::myosin heavy chain expression vector

The myosin heavy chain was encoded by an embryonic chicken myosin cDNA that had been epitope-tagged as previously described (Kinose et al., 1996; Molina et al., 1987). The GFP::myosin heavy chain fusion was constructed in the GFP expression vector pS65T-C1 (CLONTECH Laboratories, Inc., Palo Alto). The 5′ end of the GFP coding region through a unique *Pml*I restriction site was derived from the pS65T-C1 vector. The 3′ end of the GFP coding region was derived from a thermally stable, fast folding GFP variant, GFP5 (Siemering et al., 1996). This segment was amplified by PCR from the vector pcGFP5 and modified to include a six base linker sequence with a unique *Kpn*I site for fusion to the myosin coding sequence using the 5′ PCR primer CAA GGA CGA CGG GAA CTA CAA GAC and the 3′ primer CAT GGG TAC CTT GTA TAG TTC ATC CAT GCC. The 436 bp PCR product was cut with *Pml*I and *Kpn*I and cloned together with a *Kpn*I-*Bam*HI insert containing the full-length myosin heavy chain sequence into *Pml*I and *Bam*HI cut pS65T-C1. The resulting 10.6 bp vector, pGFP5-MHC (myosin heavy chain), was used as the base for all transfections and mutagenesis. The FHC mutations were introduced in the myosin coding region by PCR mutagenesis. These segments were cloned into unique restriction sites of the base expression vector then confirmed by sequencing.

Preparation and transfection of embryonic cardiomyocytes

Primary cultures of chicken cardiomyocytes were prepared from stage 26-30 white leghorn chicken embryos (Hamburger and Hamilton, 1992). The hearts were excised from 1-2 dozen embryos, the pericardium and atria were removed, and ventricular cardiomyocytes were prepared using brief trypsin treatment followed by collagenase digestion as described previously (Moncman and Wang, 1995). The top layer of the cell pellet was enriched in cardiomyocytes and was re-suspended in 5% FBS/DMEM, counted and plated at 1×10^4 cardiomyocytes/cm^2 on glass coverslips or glass-bottom 35 mm tissue culture dishes that were pretreated with 10 μg/ml of mouse EHS cell laminin (Colognato et al., 1999). Cells are maintained in 5% FBS, DMEM without glutamine at 37°C and 5% CO_2 and allowed to recover for 24 hours before transfection. For fluorescent observation, cardiomyocytes were shifted to 5% FBS in Hepes buffered DMEM/F12 medium without phenol red (Life Sciences, Gaitherburg, MD).

Expression vector DNA used in transfection assays was purified on CsCl gradients (Moncman et al., 1993) before transfection with Fugene 6 reagent (Boehringer Mannheim, Germany). The transfection mixture contained 2 μg vector DNA and 4 μl Fugene per 35 mm dish. Cells were incubated for 18 hours with this mixture then transferred to fresh medium.

Immunofluorescence microscopy and antibodies

Cells were processed for immunofluorescence 48-120 hours post-transfection essentially as described previously (Kinose et al., 1996). The cells were incubated with primary antibodies at 2 μg/μl for 1 hour at room temperature or overnight at 4°C. Rhodamine-labeled secondary antibodies were diluted 1:600 in 1% BSA, 0.05% Tween in PBS. Coverslips were washed extensively with PBS before sealing the surface to a glass slide with FITC guard mounting medium (Molecular Probes, Eugene, OR). Monoclonal antibodies (mAb) 12C5.3 and 10F12.3 react specifically with chicken skeletal muscle myosin (Winkelmann et al., 1995; Winkelmann et al., 1993). mAb F18 reacts with striated muscle myosin heavy chains (Miller et al., 1989). mAb RT11 reacts with the PEVK repeat region of titin (Moncman and Wang, 1996) and mAb N114 reacts with the cardiac specific form of nebulin (Moncman and Wang, 1995). The cardiomyocytes were sub-confluent at 72 hours post-transfection when they were fixed and stained for scoring.

Microscopy

Digital images were collected on an Olympus IX70 inverted fluorescence microscope (Olympus America Inc., Melville, NY) with a MicroMax cooled CCD camera (Roper Scientific, Princeton, NJ) using IpLab image analysis software (Scanalytics Inc., Fairfax, VA). Live cell imaging and time-lapse experiments were done with a PDMI-2 micro-incubator and perfusion pump (Harvard Apparatus Inc., Holliston, MA). The cells were plated on laminin-coated 12 mm glass coverslip inserts in 35 mm culture dishes. Differential interference contrast (DIC) images of contracting cardiomyocytes were recorded with a 100× 1.3 NA Plan Apo objective and a Hamamatsu C2400 CCD camera with an Argus 20 image processor (Hamamatsu USA Inc., Bridgewater, NJ). Digitized video sequences were collected at 30 frames/second and analyzed with IpLab image analysis software using a script for detection and tracking of z-lines.

Adenovirus vectors for expression of GFP-myosin

The complete coding regions of the WT and mutant GFP-myosin cDNAs were excised from the pGFP5-MHC vectors at unique flanking *Nhe*I and *Bam*HI restriction sites and cloned between an enhanced CMV promoter and a SV40 polyadenylation signal sequence in a modified AdEasy shuttle vector, pCMVShuttle (He et al., 1998). Recombinant adenovirus DNA was prepared by homologous recombination of shuttle vectors with the pAdEasy1 vector in *E. coli* strain BJ5183 essentially as described previously (Chow et al., 2002; He et al., 1998). Colonies were selected for kanamycin resistance and plasmid DNA was characterized by restriction digestion. The recombinant vector DNA was subcloned into *E. coli* DH10B cells and the 38 kb pAdGFP-MHC plasmid was purified by CsCl density gradient. Human 293 cells werere transfected with linearlized pAdGFP-MHC DNA as previously described (Chow et al., 2002). The recombinant adenovirus was harvested once virus plaques were evident and about 50% of the cells were rounded and detaching from the surface. Virus stocks were amplified and virus titer was determined by infection of confluent 293. Virus titers of 10^{10}-10^{11} plaque forming units (PFU)/ml were routinely achieved.

Adenovirus infection of C2C12 myotubes and preparation of GFP-myosin

Maintenance of the mouse myogenic cell line, C2C12 (CRL 1772;

American Type Culture Collection, Rockville, MD), has been described in detail elsewhere (Chow et al., 2002; Kinose et al., 1996). For isolation of GFP-myosin, myoblasts were plated on 100 mm tissue culture dishes that had been pretreated with 10 μg/ml of mouse laminin. The cells were seeded at an initial density of 7.5×10^4 cells/cm^2. Cells at 60-70% confluence were induced to differentiate by switching them to fusion medium. The cells were infected with AdGFP-MHC ~48 hours later at a multiplicity of infection (MOI) of 1000-3000 in fresh medium, and incubation was continued for an additional 24-36 hours. The medium was changed daily after infection. Myosin was isolated from 10-20 100 mm dishes of infected C2C12 myotubes as previously described (Kinose et al., 1996). Further purification by ion-exchange chromatography on a Mono Q HR5/5 column (Pharmacia, Piscataway, NJ) was done in 40 mM sodium pyrophosphate pH 7.5, 1 mM DTT, and myosin eluted with a linear 0-0.5 M NaCl gradient.

Motility assays and data analysis

The in vitro motility assay was done as described previously (Kinose et al., 1996; Winkelmann et al., 1995). An anti-subfragment 2 monoclonal antibody (anti-S2 mAb; 10F12.3) that reacts with the recombinant GFP-myosin but not the C2C12 myosin was bound to nitrocellulose-coated glass cover slips prior to incubation with the GFP-myosin for 2-4 hours in a humidified chamber at 4°C. The coverslips were washed then transferred to a 15 μl drop of motility buffer (25 mM imidazole, 25 mM KCl, 4 mM $MgCl_2$, 0.2 mM $CaCl_2$, 7.5 mM Mg^{2+}ATP, 0.5% methyl cellulose, 0.1 mg/ml glucose oxidase, 0.018 mg/ml catalase, 2.3 mg/ml glucose and 5 mM 2-mercaptoethanol, pH 7.6) containing 1 nM phalloidin-rhodamine-labeled actin and affixed to a small parafilm ring on an alumina slide with vacuum grease. This chamber was observed with a 100× Plan Apochromat (1.3 NA) objective on an Olympus BH-2 microscope. Movement of actin filaments from 1-2 minutes of continuous video was analyzed with semi-automated filament tracking programs (Bourdieu et al., 1995; Kinose et al., 1996). The trajectory of every filament with a lifetime of at least 10 frames was determined, the instantaneous velocity of the filament moving along the trajectory, the filament length, the distance of continuous motion and the duration of pauses were tabulated. A weighted probability of the actin filament velocity for hundreds of events was fitted to a Gaussian distribution and reported as a mean velocity ± standard deviation (s.d.) for each experimental condition. The myosin concentration dependence of the actin filament velocity was fit to the empirical equation, $v=v_{max}(1-e^{-m(\rho-\rho_{onset})})$ (Winkelmann et al., 1995); where ρ is surface density of myosin molecules and ρ_{onset} the minimum surface density that supports movement and m the slope. The myosin duty ratio (f) is the fraction of the ATPase cycle (t_c) that the myosin motor domain is strongly bound (t_s) to the actin filament and providing the mechanical input to drive movement ($f=t_s/t_c$). The duty ratio is derived from the relationship between sliding velocity v_{exp} and actin filament length (l) for movement of actin over a surface coated with myosin that is defined by the equation: $v_{exp}=v_o'\times\{1-(1-f)^N\}$; where N is the number of myosin heads that are powering movement and is proportional to l, and v_o' is the maximum velocity at the myosin density (Harada et al., 1990; Uyeda et al., 1990). The number of myosin heads that are available to interact with a unit length (l) actin filament, N/l, is a function of ρ, the myosin surface density (mol/μm^2). The data are best fit with a Nearest-Neighbor model that assumes the leading end of a sliding actin filament can move freely to interact with the nearest-neighboring myosin molecule along its path within a radius, r_o (Uyeda et al., 1990). This radius is a function of the surface density of randomly distributed myosin molecules and is given by:

$$N/l = 1/r_o = \sqrt{\frac{\pi\times\rho}{\ln 2}}\ .$$

The lengths and velocity of a large number of actin filaments (400-800) were sorted into 15 bins based on length, and the average filament velocity (v_{exp}) of each bin is plotted against the average filament length (l). The regression fit to the equation,

$$v_{exp} = v_o' \times \{1-(1-f)^{(l\times\sqrt{(\pi\times\rho)/\ln 2})}\}\ ,$$

is weighted by the number of filaments (n) in each bin.

Results

GFP-tagged striated muscle myosin

We were interested in investigating the effect on myofibril organization of point mutations in the myosin motor domain that are associated with familial hypertrophic cardiomyopathies. To accomplish this we have developed a GFP-tagged myosin heavy chain chimeric gene and expressed this gene in living embryonic chicken cardiomyocytes and in C2C12 myotubes. The GFP domain of the chimera contains an S65T mutation to enhance fluorescence and two additional point mutations that improve thermal stability and enhance folding (Siemering et al., 1996). The GFP coding region is fused to the 5′ end of an embryonic striated muscle myosin heavy chain cDNA (Kinose et al., 1996; Molina et al., 1987).

A model of the GFP-myosin fusion was created from the atomic coordinates of both proteins (Fig. 1). The model shows the location of the GFP with respect to key binding sites on myosin subfragment-1. The N-terminal fusion to myosin places the GFP on the surface opposite the actin-binding interface and on the same side of the motor domain as the ATPase pocket. The positions within the myosin motor domain of the three FHC mutations are highlighted. For simplicity, the mutations are referenced by the position in the human β-cardiac myosin protein sequence (R403Q, R453C and G584R) rather than the GFP-myosin sequence. These mutations are found at conserved residues that are shared by the human β-cardiac and the chicken striated muscle myosin used in this study (Rayment et al., 1995). All three mutations are associated with severe disease prognosis (Franz et al., 2001; Ko et al., 1996; Watkins et al., 1992). The R403Q mutation is in a loop near the actin-binding surface and has been studied extensively (Moss and Periera, 2000). The R453C mutation is in the switch II region of the γ-phosphate sensing mechanism of the myosin ATPase. The G584R mutation is on the relay path between the actin-binding site and the converter domain.

Transient expression of GFP-myosin in embryonic cardiomyocytes

Embryonic cardiomyocytes were isolated from ventricles of stage 26-30 chicken embryo hearts. The embryonic cardiomyocytes begin to reorganize their contractile cytoskeleton as they attach to the laminin-coated surfaces during the 24 hours recovery period before transfection with GFP-myosin expression vectors. Transient expression in about 5% of the cardiomyoctyes was routinely achieved and expression of the GFP-myosin persists for up to 2 weeks.

About 12 hours post-transfection, weak and diffuse fluorescence from the GFP-myosin is first detected. By 18-24 hours post-transfection, the GFP-myosin is found co-assembled with the endogenous myosin in non-striated myofilaments, scattered thick filaments, thick filament bundles

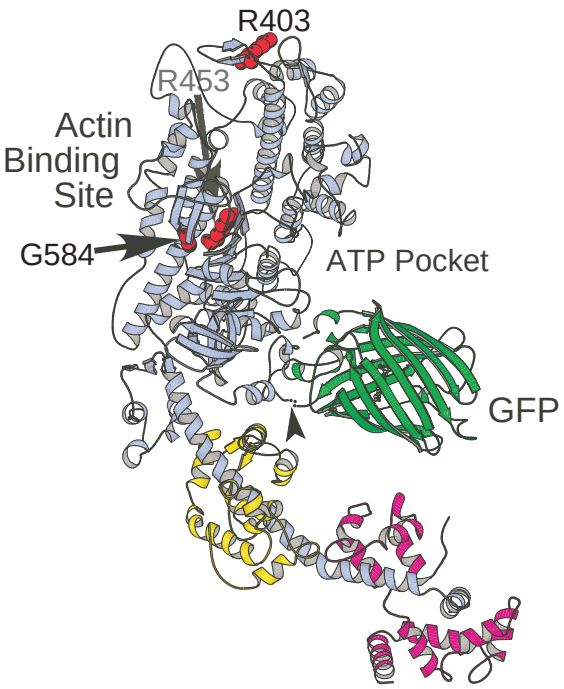

Fig. 1. A molecular model showing the location of the GFP fusion to the myosin motor domain. This ribbon representation of the myosin motor domain (blue) and GFP (green) illustrates the linkage (arrowhead) of the C terminus of GFP to the N terminus of myosin. This model illustrates the important functional sites on the myosin motor domain in relation to the GFP attachment point. The three point mutations in the motor domain (R403Q, R453C and G584R) are identified with CPK models (red) of the WT residues. The essential light chain (yellow) and the regulatory light chain (magenta) are bound to the myosin lever arm. Model coordinates are for adult pectoralis muscle myosin subfragment-1 (Rayment et al., 1993) and GFP (Yang et al., 1996).

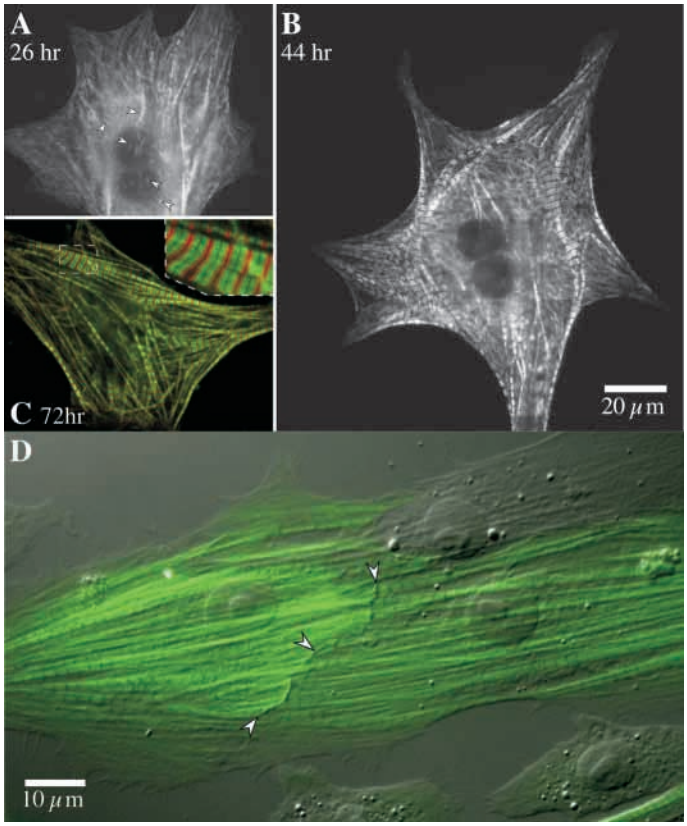

Fig. 2. Transient expression and assembly of GFP-myosin in embryonic cardiomyocytes. (A) In this live cardiomyocyte imaged 26 hours post-transfection the GFP-myosin is found assembled in striated myofibrils, in non-striated myofilaments, and in scattered thick filaments (white arrowheads) and non-aligned A-bands. (B) The same cell was examined 18 hours later (44 hours post-transfection). The organization and number of myofibrils in the cell have increased with a concomitant decrease in the non-striated fluorescence. (C) A cardiomyocyte expressing GFP-myosin (green) was fixed 72 hours post-transfection and stained with mAb RT11 (red) that labels the titin PEVK domain at the A-I junction (Moncman and Wang, 1996). The boxed region is enlarged (inset) to show the ordered myofibril structure. (D) A DIC image overlaid in green with the fluorescent image of GFP-myosin. Two adjacent cells are expressing GFP-myosin and a third neighboring cell is not. The GFP-myosin-expressing cells have formed a prominent intercalated disk (white arrowheads) and the myofibrils are arranged co-linearly across the disk. The magnification in A-C is the same.

and striated myofibrils (Fig. 2A). As the cells spread and establish new substrate attachments, there is an increase in the number of myofibrils and the degree of organization in many of the cells. The cell that is shown at 26 hours post-transfection (Fig. 2A) was observed again 18 hours later (Fig. 2B). The GFP-myosin has incorporated into the contractile cytoskeleton resulting in a decrease in the non-striated fluorescence that was apparent earlier and an increase in fluorescence intensity from the GFP-myosin that has incorporated into the re-assembled contractile cytoskeleton. The cardiomyocytes beat spontaneously throughout the process.

The re-organization of the contractile cytoskeleton is complete by 72 hours post-transfection (Fig. 2C). In this example, the GFP-myosin is uniformly incorporated into the contractile units of myofibrils in well defined, 1.6 μm long, periodic A-bands with clear bare zones. Immunostaining for other contractile proteins including cardiac titin (Fig. 2C), myosin, nebulette and actin show that they compliment the organization of the GFP-myosin. Ordered and contracting myofibrils are observed in over two-thirds of the transfected cardiomyocytes expressing GFP-myosin. A similar degree of organization is seen in non-transfected cardiomyocytes after they are fixed and stained for myofibril proteins (data not shown).

In addition to re-assembling the contractile cytoskeleton, embryonic cardiomyocytes that are in close proximity establish cell-cell interactions. These include intercalated disks between neighboring cells that can be visualized with DIC optics as seen in Fig. 2D. In this example, two adjacent transfected cells and a third non-transfected cell have come together. A well-defined intercalated disk is apparent between the two GFP-

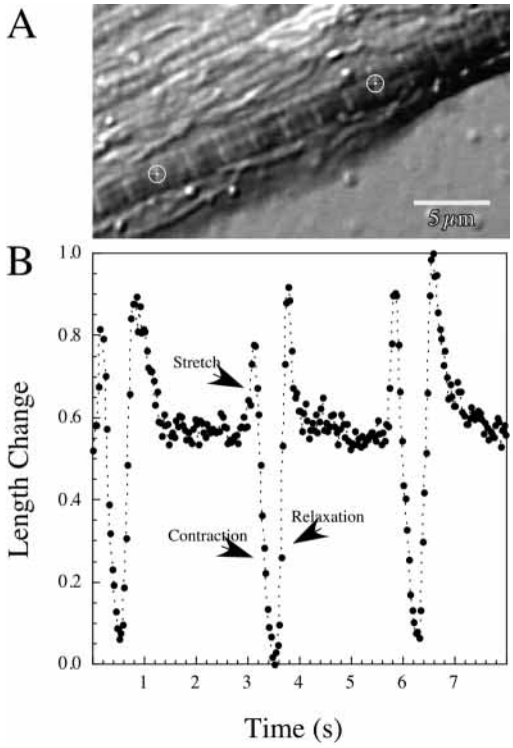

Fig. 3. The contractile activity of GFP-myosin-expressing cells. (A) DIC image of a small area of an R403Q mutant GFP-myosin-expressing cardiomyocyte showing a clearly defined myofibril. Two *z*-lines spaced 7 sarcomeres apart are marked with small bulls eyes. The fluorescent cell was selected then the DIC image was recorded at 30 frames/second. (B) The positions of the two marked *z*-lines were tracked over time and the relative length changes plotted. The velocities of the contraction and relaxation phases (*d*L/*d*T) were determined and summarized in Table 1. Cells were maintained at 30°C on a heated microscope stage. Movies of this cell and another can be found at http://jcs.biologists.org/supplemental.

myosin-expressing cells. The myofibrils in these two cells have assembled co-linearly across that boundary. These cells are mechanically coupled and beat in unison.

The combined DIC and fluorescent image also shows that the GFP-myosin is only assembled into the contractile cytoskeleton. The contractile myofibrils and the GFP-myosin are not found near the very edge of the cell, a domain reserved for the non-muscle cytoskeleton. These observations indicate that the GFP-myosin chimera co-assembles faithfully with the endogenous cardiac myosin in embryonic cardiomyocytes and contributes to the re-establishment of the contractile phenotype of these cells.

Contracting embryonic cardiomyocytes

Cardiomyocytes prepared by relatively mild collagenase disruption of early stage chicken embryo hearts beat spontaneously throughout their isolation and re-organization in vitro and continue to beat for days in culture (Moncman and Wang, 1995; Moncman and Wang, 2002). Transfection of the cardiomyocytes and GFP-myosin expression does not interfere with this activity. The contraction of individual cells was monitored by fluorescence and DIC microscopy (Fig. 3). The velocity of contraction was measured 72-120 hours post-transfection in individual cells expressing the WT and mutant GFP-myosin. The distance between Z-lines separated by 4-12 sarcomeres within a contracting myofibril was tracked over time using an automated edge detection algorithm (Fig. 3A). The beats are often characterized by an initial stretch activation followed by contraction and relaxation phases (Fig. 3B). The stretch activation is provided by an adjacent beating cardiomyocyte.

Table 1. Contractile activity of embryonic cardiomyocytes expressing GFP-myosin

Sample	Number of cells	Sarcomere length (μm)	Contraction (μm/s)	Relaxation (μm/s)
Non-transfected	7	2.07±0.15	0.43±0.17	0.52±0.31
WT GFP-myosin	15	2.04±0.26	0.49±0.30	0.52±0.31
R403Q	21	1.98±0.18	0.41±0.22	0.55±0.41
R453C	4	2.19±0.09	0.40±0.25	0.37±0.33
G584R	6	2.28±0.16	0.42±0.22	0.60±0.05

The velocity of contraction and relaxation of individual cardiomyocytes was determined from the first derivative (*d*L/*d*T) of the time course of length changes. Cells expressing GFP-myosin were analyzed 72-120 hours post-transfection at 30°C. The mean resting sarcomere length, speed of contraction and relaxation are tabulated with the standard deviation (s.d.) for the indicated number of cells in each group. The differences in the velocity of contraction and relaxation between groups are not significant ($P<0.05$) considering the variation among cells within a group.

The velocity of the contraction and relaxation phases was measured in non-transfected cells and in cells expressing the WT GFP-myosin and the three mutants (Table 1). The analysis did not reveal a significant variation ($P<0.05$) in the velocity of contraction or relaxation between the groups. These data suggest that WT GFP-myosin and the mutants do not have a dramatic effect on the spontaneous contractions of the embryonic cardiomyocytes. However, this analysis did reveal a significant variation among the four GFP-myosin vectors in the number of well-ordered cardiomyocytes that were suitable for the measurement. Far fewer well ordered cells were available for the R453C and G584R mutants at 72-120 hours post-transfection than with the WT GFP-myosin or the R403Q mutant. This prompted an evaluation of the organization of the contractile cytoskeleton in transfected cells expressing the WT and mutant GFP-myosin.

FHC mutations disrupt the organization of the contractile cytoskeleton

Live cardiomyocytes expressing GFP-myosin can be grouped on the basis of the organization of the contractile cytoskeleton. We developed a classification scheme consisting of four levels of organization: Non-striated, Striated-1, Striated-2 and Striated-3 (Fig. 4). Cells classified as Non-striated contain brightly fluorescent myofilaments but lack organized repeating units characteristic of myofibrils. In contrast, all of the striated classes contain myofibrils but differ from each other in the level of myofibril order. Cells in the Striated-1 class contain a mixture of non-striated filaments interspersed with striated myofibrils. The myofibrils in this class are thin and are not well aligned or organized, but they do contain sarcomeric repeating units. Cells in the Striated-2 class contain extensive striated myofibrils and little or no non-striated myofilaments but have

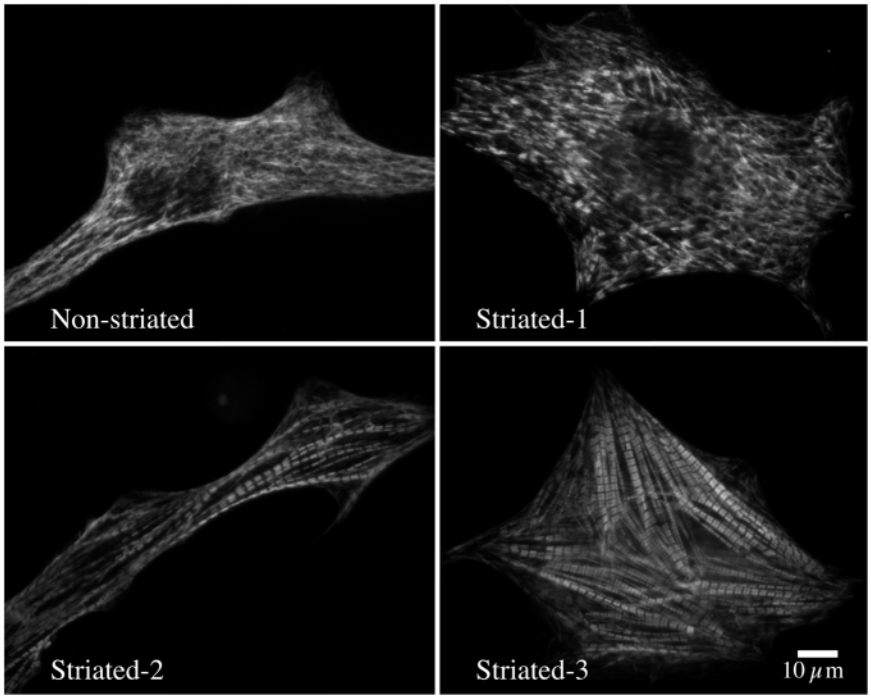

Fig. 4. Organization of the contractile cytoskeleton in transfected cardiomyocytes. The transfected cardiomyocytes can be grouped into four classes based on the degree of organization of the contractile cytoskeleton. Non-striated cells contain brightly fluorescent myofilaments but lack the organized repeating units characteristic of myofibrils. Striated-1 cells contain a mixture of non-striated myofilaments interspersed with thin and misaligned striated myofibrils. Striated-2 cells contain predominantly striated myofibrils; however, this class lacks lateral alignment of the myofibrils. Striated-3 cells are packed with laterally aligned striated myofibrils that stretch between cell attachment points. The magnification is the same in all four panels.

poor lateral alignment of the individual myofibrils. Cells in the last class, Striated-3, are packed with large, laterally aligned myofibrils that stretch between cell attachment points. This is the best outcome of the reorganization of the contractile cytoskeleton and this is the type of cells used for the contraction analysis (Fig. 3).

With a set of criteria for evaluating the organization of the contractile cytoskeleton, the effect of the transfection and expression of WT and mutant GFP-myosin was evaluated. Cells were transfected with the GFP-myosin vectors and fixed 72 hours after transfection. By this time, the attachment, spreading and reassembly of the contractile cytoskeleton of the cardiomyocytes is complete. After fixation, the cells were counterstained with an anti-titin mAb followed by rhodamine labeled secondary antibody to assist in the scoring the contractile cytoskeleton. Fibroblasts do not stain positive with the anti-titin mAb, so it was possible to exclude transfected fibroblasts from the analysis. Non-transfected cells were scored after staining with a striated muscle-specific anti-myosin mAb. To limit bias in the interpretation of the results, slides were prepared, coded and scored blind.

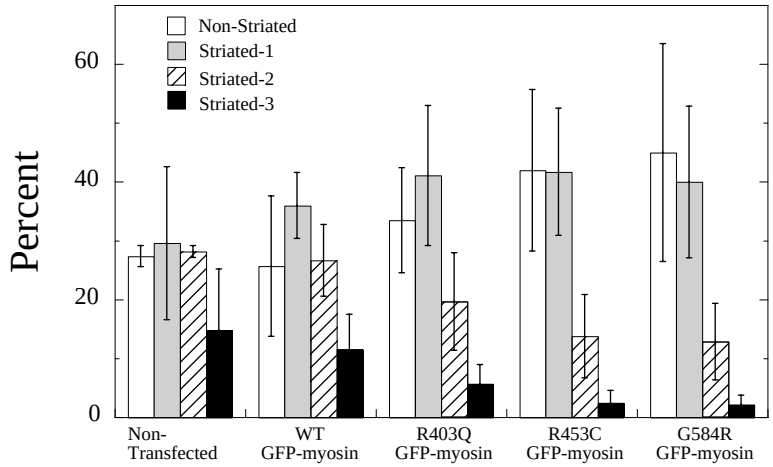

Fig. 5. Analysis of the organization of the contractile cytoskeleton in embryonic cardiomyocytes. Cells were transfected with the WT GFP-myosin and the three FHC mutants and fixed 72 hours post-transfection. The fixed cells were counter-stained with antibodies to muscle specific markers (either anti-titin, RT11, or anti-myosin, F18). The GFP-myosin-positive cells were scored in one of the four classifications illustrated in Fig. 4 and described in the text. The counterstaining for other muscle-specific protein was used to confirm the myofilament organization. The non-transfected control cells were scored after staining with anti-titin or anti-myosin. These data summarize the results from four separate experiments and include over 4400 cells. The number of cells in each group varied between 200-400 cells for a total of ~1100 cells/experiment. Pairwise comparison of the distribution of cells in classes for the different groups was done using Student's *t*-test with a confidence level of $P<0.05$. Error bars correspond to the standard deviation within each class of the four experiments.

The results of the classification are presented as a histogram representing the distribution of the cells in each of the four classes (Fig. 5). Over 4400 cells were scored from four independent transfections. In non-transfected cells about 27% of the cardiomyocytes were scored as Non-striated indicating that they did not re-assemble clearly delineated myofibrils. The remaining 73% of the cardiomyocytes contained varying degrees of ordered myofibrils and were scored in the three striated categories. Classification of the cells expressing WT GFP-myosin yielded a distribution that is indistinguishable in all four classes ($P<0.05$) from the non-transfected cells.

The cells expressing the R403Q myosin mutation show a slight but significant ($P<0.05$) decrease in the Striated-3 class that is compensated by increases in the other classes, particularly the Non-striated class ($P<0.05$), when compared to the non-transfected control and WT GFP-myosin-expressing cells. The R453C and G584R mutants both show a dramatic increase in the Non-striated class ($P<0.05$) reflecting a decrease in cells containing the most highly organized myofibrils (Striated-2 and -3 classes) ($P<0.05$). These two mutations appear to disrupt the

reassembly of the contractile cytoskeleton at the level of the lateral alignment and organization of the myofibrils. The difficulty noted earlier in finding cells for measuring the contractile activity of these two mutants is clearly reflected in the decrease in the Striated-3 class.

Thus, it appears that WT GFP-myosin participates fully in the reorganization of the contractile cytoskeleton of the embryonic cardiomyocytes. However, the FHC mutations R453C and G584R and to a lesser extent even the R403Q mutation disrupt this process leading to decreased levels of myofibril organization in actively beating embryonic cardiomyocytes.

Adenovirus expression of GFP-myosin in C2C12 cells

The expression of the GFP-myosin in live cardiomyocytes enabled us to evaluate the effect of the FHC mutations on the organization of the contractile cytoskeleton; however, we were unable to establish a direct effect of the FHC mutations on the contractile activity of these cells. A biochemical analysis of the motor activity of GFP-myosin isolated from the transfected cardiomyocytes is desirable but technically not feasible. The number of cardiomyocytes that can be isolated is relatively small, and the low efficiency of transfection of these primary cells severely limits the amount of protein that can be prepared. To evaluate the motor activity of the GFP-myosin and FHC mutants we turned to expression of GFP-myosin in C2C12 myotubes, a mouse myogenic cell line that has been useful for analysis of recombinant striated muscle myosin (Kinose et al., 1996).

We have used replication defective adenovirus capable of efficient delivery of the large GFP-myosin genes to differentiated myotubes to express GFP-myosin (Chow et al., 2002). The GFP-myosin coding regions were excised from the transient expression vectors, moved into AdEasy shuttle vectors and recombinant adenovirus stocks were prepared (He et al., 1998). With a multiplicity of infection of 1000-3000, the GFP-myosin gene can be effectively delivered to C2C12 myotubes (Chow et al., 2002). A major advantage of this approach is that the C2C12 myoblasts can be expanded to produce enough myotubes for isolation of the contractile proteins.

The WT GFP-myosin incorporates into the striated myofibrils of the multinucleated myotubes (Fig. 6). The contractile cytoskeleton becomes very well ordered, but these cells do not spontaneously contract like the embryonic cardiomyocytes. Close examination of live myotubes expressing GFP-myosin reveals a continuous oscillatory motion of the contractile units that may be involved in lateral alignment of the sarcomeres in adjacent myofibrils (see Movies at http://jcs.biologists.org/supplemental). Eventually, the large myotubes begin to actively contract, but this is often destructive to the cell layer and every effort is made to harvest the cells before this activity begins.

Since the recombinant GFP-myosin assembles with the C2C12 myosin in striated myofibrils, it is readily isolated with the endogenous myosin using standard extraction and fractionation methods (Kinose et al., 1996). Analysis of partially purified myosin from uninfected myotubes and those infected with a GFP-myosin-expressing adenovirus reveals the GFP-myosin heavy chain migrating at about 250 kDa, just above the C2C12 myosin heavy chain (Fig. 7A). The isolated myosin has a stoichiometric complement of myosin light chains. Purification of the myosin by ion-exchange chromatography removes the remaining contaminant bands, but does not separate the GFP-myosin from the endogenous C2C12 myosin (Fig. 7A). On a lower percentage acrylamide gel, the GFP-myosin heavy chain can be resolved from the endogenous C2C12 myosin (Fig. 7B). Western blotting with a mAb that recognizes an epitope on the recombinant myosin demonstrates that the upper 250 kDa band is the GFP-myosin heavy chain.

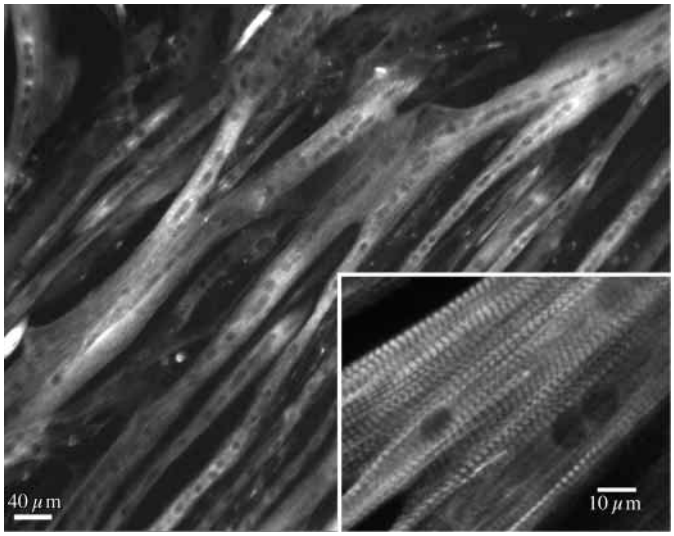

Fig. 6. Replication-defective adenovirus induced expression of GFP-myosin in C2C12 myotubes. Post-mitotic C2C12 myocytes were infected ~48 hours after transfer to fusion medium and maintained in culture for an additional 4 days. Almost all of the large myotubes are brightly fluorescent from the expressed GFP-myosin. When viewed at higher magnification (inset) it is clear that the WT GFP-myosin has assembled with the endogenous C2C12 myosin into ordered striated myofibrils.

Myosin was prepared from cells expressing the WT GFP-myosin and three FHC mutants and the levels of expression compared (Fig. 7C). The amount of recombinant GFP-myosin produced in this experiment ranged from 25-40% of the total myosin. The FHC mutations do not interfere with expression or isolation of the GFP-myosin from myotubes. However, there are subtle effects of the FHC mutations on myofibril organization in C2C12 myotubes. We did not attempt to evaluate this effect because of the large size of the multinucleated cells and resulting difficulty in defining a classification scheme for scoring cells that often span many microscopic fields.

Since the GFP-myosin and C2C12 myosin are expressed in the same cells, it is possible that the heavy chains can mix and form heterodimers. To address this question, native GFP-myosin was immunoprecipitated with a pair of mAbs that uniquely recognizes epitopes on the recombinant myosin (Fig. 7D). If heterodimers of GFP-myosin and C2C12 myosin exist, then a significant amount of the C2C12 myosin would be expected to co-precipitate since this heavy chain is in 1.5- to 3-fold excess over the GFP-myosin. However, the level of C2C12 myosin that precipitates with the four GFP-myosin

samples is only slightly higher than the level that precipitated non-specifically from the uninfected control C2C12 myosin sample. The GFP-myosin is predominantly (>90%) a heavy chain homodimer.

Motor activity of GFP-myosin FHC mutants

The motor activity of the GFP-myosin was measured with an in vitro motility assay. An anti-S2 mAb that reacts with the GFP-myosin but not with the C2 myosin was used to selectively tether the recombinant myosin to antibody-coated glass coverslips (Kinose et al., 1996; Winkelmann et al., 1995). The velocity of actin filament movement is dependent on the surface density of motors, so the myosin concentration dependence of the actin velocity was examined. The WT GFP-myosin moves actin filaments at 4.00±0.25 μm/s (Fig. 8). This is in close agreement with the speed measured for the same embryonic striated muscle myosin lacking the GFP tag (Kinose et al., 1996), when rates are corrected for the difference in temperature for the two measurements. This indicates that the GFP tag on the embryonic myosin does not interfere with the myosin motor activity.

The analysis of the motor activity of the three FHC mutations reveals a variety of interesting changes. The R403Q mutation increases (P<0.05) the velocity of actin filament movement (4.30±0.30 μm/second). This mutant also appears to require higher myosin concentrations to achieve the maximum filament velocity. The other two FHC mutations both decrease the actin filament velocity. The R453C mutation slows the actin filament velocity by over 60% (1.45±0.22 μm/second) and the G584 mutation slows the velocity by 40% (2.41±0.13 μm/second) compared to the WT GFP-myosin. The

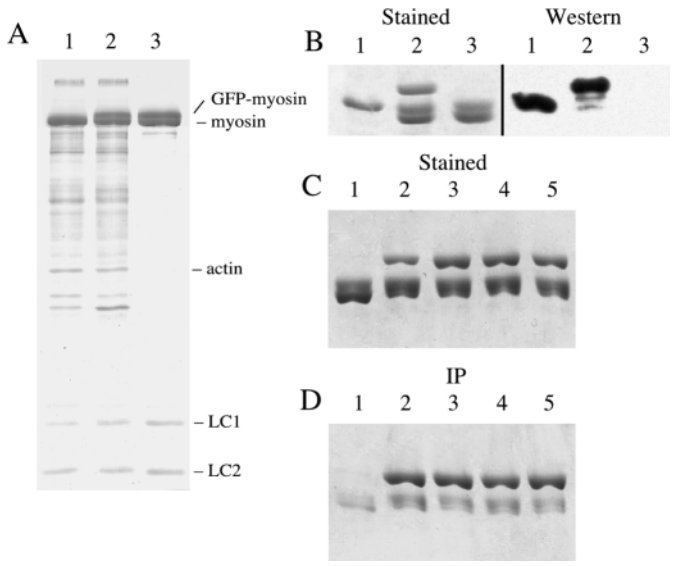

Fig. 7. Isolation and analysis of the GFP-myosin expressed in C2C12 myotubes. (A) SDS-PAGE of myosin isolated from uninfected C2C12 myotubes (lane 1), myotubes infected with WT AdGFP-MHC and expressing GFP-myosin (lane 2), and purified GFP-myosin sample after ion-exchange chromatography (lane 3). The myosin heavy and light chains are resolved in this 12.5% acrylamide gel. The GFP-myosin heavy chain migrates just above the C2C12 myosin heavy chain in lane 2. (B) A 6% acrylamide gel clearly resolves the GFP-myosin heavy chain from the C2C12 myosin heavy chain: lane 1 – Purified adult chicken pectoralis muscle myosin; lane 2 – myosin isolated from infected C2C12 cells; lane 3 – Myosin from uninfected C2C12 myotubes. A western blot of the same samples developed with mAb 12C5.3 that selectively reacts with the chicken muscle myosin and labels the 250 kDa GFP-myosin heavy chain, but does not detect the C2C12 myosin. (C) SDS-PAGE analysis of myosin isolated from C2C12 myotubes of uninfected cells (Lane 1), and cells expressing WT GFP-myosin (Lane 2), R403Q (Lane 3), R453C (Lane 4) and G584R (Lane 5). These cells were harvested 96 hours post-infection. Densitometry of the stained gel reveals that the GFP-myosin amounts to 25-40% of the total myosin from the infected myotubes. (D) Immunoprecipitation of the GFP-myosin under native conditions with two anti-myosin mAbs (12C5.3 and 10F12.3) that uniquely recognize the chimeric GFP-myosin reveals that the chimeric protein is predominantly a homodimer.

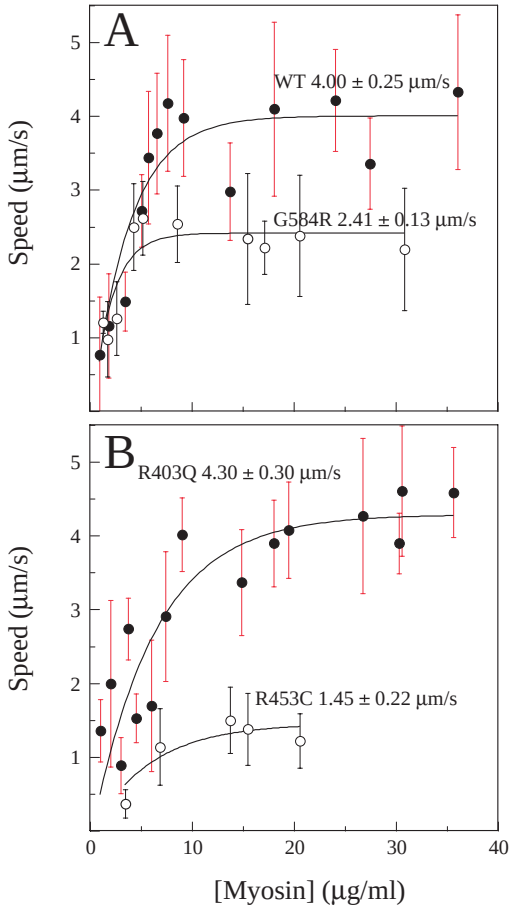

Fig. 8. The myosin concentration dependence of the actin filament velocity measured in an in vitro motility assay. (A) The velocity of actin filament was measured on antibody capture surfaces incubated with various concentrations of WT and G584R myosin. The velocity of sliding movement at saturating myosin surface density is indicated. (B) The R403Q and R453C data are plotted and the actin filament velocity is indicated. The data points correspond to the mean (±s.d.) for a Gaussian distribution of the actin filament velocity at each myosin concentration tested (Kinose et al., 1996). The myosin concentration dependence of the actin filament sliding velocity was fit to the empirical equation: $v=v_{max}(1-e^{-m(\rho-\rho_{onset})})$. The GFP-myosin concentration was determined by densitometry of stained SDS gels and fluorescence spectroscopy. Actin filament motility was measured at 30°C.

G584R mutation also appears to achieve the maximum actin filament velocity at lower myosin concentrations than the WT GFP-myosin.

The actin filament length dependence of the velocity is obtained from the motility assay. These data can be used with the myosin surface density to estimate the duty ratio for the myosin mechano-chemical cycle (Harada et al., 1990; Uyeda et al., 1990). The duty ratio (*f*) is the fraction of the ATPase cycle that the myosin motor domain is strongly bound to the actin filament and providing the mechanical input to drive movement. The binding of GFP-myosin to the surfaces used for motility assays can be measured directly by fluorimetry (Fig. 9A). The binding curve from the fluorescence titration fitted previous binding measurements (Winkelmann et al., 1995) and provided a rapid method for determining the myosin surface density. The myosin surface density and the actin filament length/velocity relationship were used to estimate the myosin duty ratio for the WT and mutant GFP-myosin (Fig. 9B).

The duty ratio for the WT GFP-myosin and the R403Q mutant are the same; the myosin is tightly bound to actin for 2% of the ATPase cycle (Table 2). The R453C and the G584R mutants both had a higher duty ratio (~4%) indicating that they are tightly bound to actin for a longer fraction of the myosin ATPase cycle. The analysis of the GFP-myosin motor activity indicates that the FHC mutations affect the unloaded shortening velocity and myosin duty ratio. The magnitude of these changes in motor activity qualitatively mirrors the effects that these mutations have on the reassembly of the contractile cytoskeleton in embryonic cardiomyocytes.

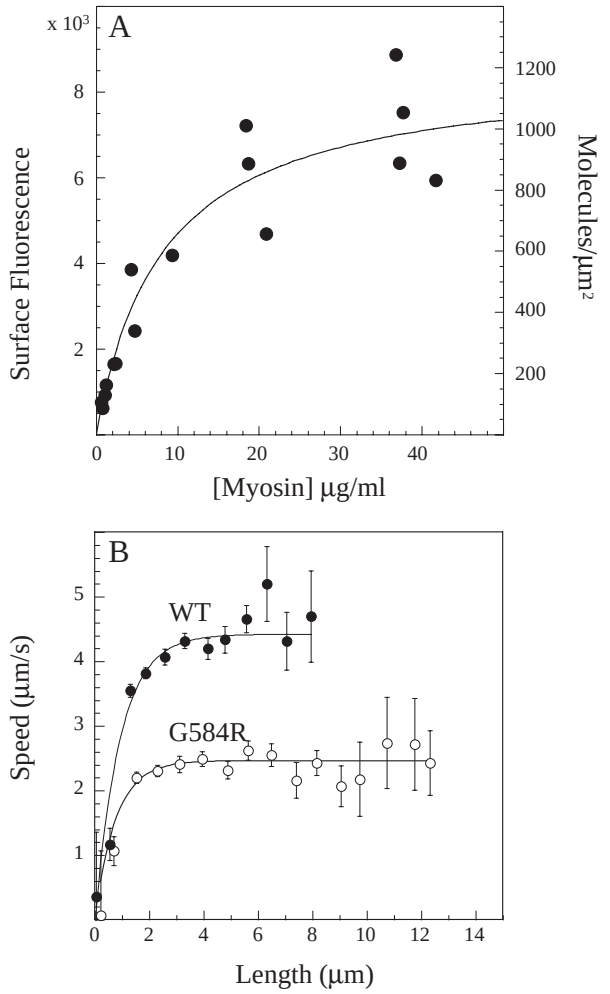

Fig. 9. Myosin surface density determination and actin filament length dependence of unloaded shortening velocity. (A) Fluorescent quantitation of the binding of GFP-myosin to mAb-coated glass coverslips. The fluorescence from GFP-myosin bound to the surface was measured by placing the coverslip at a 45° angle to the light path in motility buffer in a standard 1 cm cuvette. The solid line is a fit of the myosin concentration dependence of iodinated adult skeletal muscle myosin binding to the mAb surfaces (Winkelmann et al., 1995). This provides a rapid method for determining the myosin surface density used in the in vitro motility assay. (B) Actin filament length dependence of the unloaded shortening velocity was used to estimate the duty ratio for WT and mutant GFP-myosin. The sliding filament velocity (v_{exp}) and actin filament length (l) data were fit to the equation

$$v_{exp} = v_o' \times \{1 - (1 - f)^{(l \times \sqrt{(\pi \times \rho)/\ln 2})}\}$$

for each myosin surface density (ρ) (Harada et al., 1990; Uyeda et al., 1990). The data is weighted by the number of filaments (n) in each length bin. This is indicated for each data point by the vertical bars that are equal to $1/n^{1/2}$. These data are for WT GFP-myosin at a myosin surface density of 830 mol/μm^2 and the G584R mutant at 414 mol/μm^2.

Discussion

GFP-myosin as a probe for myosin assembly and activity

We designed and constructed a GFP::myosin fusion protein to follow the expression and assembly of myosin in live muscle cells. Fusion of GFP to the N terminus of the myosin heavy chain does not interfere with myosin filament assembly or motor activity. The WT GFP-myosin participates fully in the re-organization of the contractile cytoskeleton of embryonic cardiomyocytes. The myosin heavy chain used as the basis of these expression experiments was originally cloned from early embryonic chicken breast muscle (Kinose et al., 1996; Molina et al., 1987). The myosin gene (N118) is expressed in early embryonic chicken skeletal muscle and cardiac muscle and expression persists into the adult in both cardiac and skeletal muscle (Kropp et al., 1987; Molina et al., 1987). In some ways,

Table 2. Summary of GFP-myosin motor activity

Sample	Actin filament velocity (μm/s)	Duty ratio
WT GFP-myosin	4.00±0.25	0.020±0.003
R403Q	4.30±0.30	0.020±0.004
R453C	1.45±0.22	0.038±0.001
G584R	2.41±0.13	0.038±0.012

Comparison of the actin filament velocity measured in the motility assay and the myosin duty ratio derived from the analysis of the movement data for WT GFP-myosin and the FHC mutations. The duty ratio is the mean for measurements at three myosin surface densities for each sample covering a range of 400-1000 myosin molecules/μm^2 (± s.d.). The actin filament velocity (v_{max}) is derived from the fit of the data in Fig. 8 with the error for that fit. The FHC mutations (R453C and G584R) that strongly disrupt the reorganization of the contractile cytoskeleton in embryonic cardiomyocytes have strong effects on the unloaded shortening velocity measured in the motility assay and on the myosin duty ratio.

the chicken N118 gene is like the human β-cardiac gene in that it is expressed in both skeletal and cardiac muscle (Cuda et al., 1993; Fananapazir et al., 1993; Lankford et al., 1995).

The transient expression of WT GFP-myosin in embryonic cardiomyocytes persists for up to 2 weeks in culture. Throughout this period the embryonic chicken cardiomyocytes beat spontaneously. The excitation-contraction coupling system is not well developed in early embryonic cardiomyocytes and spontaneous contractions are triggered by intracellular Ca^{2+} oscillations (Rabkin, 1993; Viatchenko-Karpinski et al., 1999). Expression of WT and FHC mutant GFP-myosin does not disrupt this spontaneous activity. The velocity of contraction and relaxation was measured and is comparable for non-transfected cells and cells expressing the WT GFP-myosin and the FHC mutants. The load imposed by substrate attachment and interactions between cells can have a large effect on the contraction velocity. It was not controlled in these experiments. Consequently, there is significant variation in shortening velocity between the cells within each experimental group that overshadows differences between groups. Although we were unable to discern differences in contractile activity, this analysis does demonstrate that these cells do actively contract throughout the course of the transient expression experiment, and the FHC mutations do not block this activity.

Analysis of assembly defects associated with FHC mutations

We have demonstrated that actively contracting cardiomyocytes expressing GFP-myosin with FHC mutations (R403Q, R453C and G584R) exhibit significant disorganization of the contractile cytoskeleton. In contrast, the WT GFP-myosin did not disrupt the myofibril organization. The R403Q mutation had an effect on the number of cells that were most highly ordered, the Striated-3 class, with a shift of cells in this class to the other three classes. Overall this mutation had the smallest effect on the myofibril organization of the three FHC mutations. The R453C and G584R mutations have more dramatic effects on all striated classes, reducing the level of organization and increasing the degree of myofibril disarray. Thus, expression of all three FHC mutations disrupts the organization of the contractile cytoskeleton of embryonic cardiomyocytes.

The morphology and the contractile function of left ventricular cardiomyocytes isolated from wild-type and heterozygous α-$MHC^{R403Q/+}$ mutant transgenic mice has been analyzed (Kim et al., 1999). Examination of the α-$MHC^{R403Q/+}$ cardiomyocytes revealed far fewer highly ordered cardiomyocytes with well-aligned, parallel myofibrils than the wild-type control group and many more shorter, fatter cardiomyocytes with disorganized myofibrils. The α-$MHC^{R403Q/+}$ cardiomyocytes had impaired rates of contraction and relaxation that correlated with the degree of myofibril disorder. It was concluded that the impaired function was due, at least in part, to the morphological abnormalities of the cells expressing the mutant myosin. This is consistent with a direct effect of the R403Q myosin mutation on the organization of the contractile cytoskeleton leading to a defect in cardiomyocyte and global cardiac function.

Others have reported mixed results for the effect of myosin mutations on myofibril organization in myocytes. Epitope-tagged WT and mutant human β-cardiac myosin were transiently expressed in neonatal rat ventricular cardiomyocytes (Becker et al., 1997). A mutation in the myosin ATPase site (K184R) that blocks nucleotide exchange and produces a rigor-like interaction with actin dramatically disrupts myofibril reassembly in the neonatal cardiomyocytes. However, two FHC mutations (R403Q and R249Q) and a mutation that may inhibit myosin motor activity (S472V) had no effect on the organization of the contractile cytoskeleton of the neonatal cardiomyocytes. Similarly, the expression of three β-cardiac myosin FHC mutants (N232S, G741R and D778G) in cultured skeletal muscle myotubes had little effect on myofibrillogenesis (Miller et al., 2000).

Our results with the expression of the WT GFP-myosin and FHC mutants in C2C12 myotubes is consistent with the conclusion that they do not dramatically disrupt myofibrillogenesis in cultured myotubes even when expressed at 25-40% of the total myosin in those cells. Subtle differences in the organization of the myofibrils in myotubes expressing FHC mutants were observed but not scored here. The disorder did not appear to influence isolation of the expressed myosin. There are enormous differences between the contractile cytoskeleton of the large multinucleated myotubes and the mono- and di-nucleate cardiomyocytes. These include differences in the mechanical activity of embryonic cardiomyocytes when compared to both cultured myotubes and neonatal rat cardiomyocytes. The embryonic chick cardiomyocytes are actively contracting throughout the re-organization of the contractile cytoskeleton and the incorporation of the myosin mutants into that cytoskeleton. The cultured myotubes and the neonatal rat cardiomyocytes do not exhibit this type of spontaneous contractile activity. Expression of GFP-myosin in live C2C12 myotubes reveals that sarcomeres are in constant asynchronous oscillatory motion (see Supplemental data: http://jcs.biologists.org/supplemental). This activity may be essential for lateral alignment and organization of the contractile cytoskeleton, but it is very different from the spontaneous beating of the embryonic cardiomyocytes.

Myosin activity is important for the assembly and stabilization of the contractile cytoskeleton in muscle (Eble et al., 1998), and some level of activity is required for the proper assembly of myosin in cardiomyocytes and cultured myotubes (Moncman and Wang, 2002; Ramachandran et al., 2003; Soeno et al., 1999). The complete inhibition of myosin motor activity by a mutation (K184R) that induces a rigor-like state may explain the dramatic disruptive effect that this myosin has on the re-assembly of the contractile cytoskeleton of the neonatal rat cardiomyocytes (Becker et al., 1997). However, less dramatic mutations that modulate myosin motor activity such as the FHC mutation may not disrupt myofibril organization in the absence of active contractions.

The FHC mutations affect the myosin motor activity

The isolated GFP-myosin has motor activity comparable to a non-GFP-tagged form of this myosin indicating that the GFP domain does not disrupt motor activity (Kinose et al., 1996). All three of the FHC mutations affect the sliding velocity of actin filaments. The R403Q mutation has the least dramatic

effect showing a small increase (~10%) in actin filament velocity. This is accompanied by an increase in the myosin surface density necessary to saturate the sliding filament speed, suggesting a weaker interaction of R403Q myosin with actin filaments. Increased actin filament velocity is consistent with a decrease in the duration of the force generating state (t_s). The duty ratio of the R403Q mutant did not change compared to WT suggesting that both the duration of the force generating state (t_s) and the ATPase cycle time (t_c) may have decreased for this mutant, leaving the ratio constant. This would enhance filament velocity but diminish force production by the R403Q myosin.

The R453C and G584R mutations have greater affects on the myosin motor activity resulting in a 40-60% decrease in the actin filament velocity. The G584R mutation appears to reach the maximum velocity at lower myosin surface densities consistent with a stronger interaction with actin. Both the G584R and R453C mutations increase the duty ratio suggesting that myosin spends a greater fraction of the ATPase cycle strongly bound to actin. A higher duty ratio can give rise to a lower unloaded shortening velocity and an increased average force. The effect of all three mutations on myofibril organization suggests that incorporation of myosin with both enhanced and diminished motor activity can perturb the balance of forces at the level of the sarcomere and contribute to myofibril disarray in the actively beating cardiomyocytes.

A number of other groups have measured the sliding filament velocity of the R403Q mutation using myosin isolated from heterologous expression systems or biopsies of FHC patients. Some of the earlier measurements detected a decreased rate of sliding filament velocity (Cuda et al., 1997; Fujita et al., 1997; Sweeney et al., 1994). However, more recent measurements with human β-cardiac, mouse α-cardiac and smooth muscle myosin all suggest a gain of function with increased sliding filament velocity (30% to >200%), accelerated actin-activated myosin ATPase activity and decreased actin affinity (Palmiter et al., 2000; Tyska et al., 2000; Yamashita et al., 2000). These later results are consistent with the increased filament velocity and decreased actin affinity that is reported here for R403Q myosin. The R453C and G584R mutations have not been as extensively studied. One report of the G584R mutation engineered into *Dictyostelium* myosin measured a reduced sliding filament velocity (Fujita et al., 1997) consistent with that reported here.

The magnitude and direction of change that these mutations have on the myosin motor activity may be dependent on the specific myosin isoform under study. This is particularly true if the changes are modulating the kinetics of the myosin interaction with actin (Moss and Periera, 2000; Tyska et al., 2000). However, in the experiments presented here we have shown a correlation between the changes in motor activity of FHC mutations in the same myosin backbone as was used to evaluate myofibril organization in isolated, actively contracting cardiomyocytes. This leads to the conclusion that FHC mutation that affects myosin motor activity can disrupt myofibril organization in active cardiomyocytes in the absence of other contributing factors.

The authors wish to acknowledge the assistance of Ying Chen and Dr Michael Sanders at various stages of this work. The authors are indebted to Drs Jean Schwarzbauer and Rajani Srikakulam for advice and critical reading of this manuscript and Dr Chavela Carr for use of the fluorometer. This work was supported by PHS grant AR38454 and the New Jersey Commission on Science and Technology.

References

Becker, K. D., Gottshall, K. R., Hickey, R., Perriard, J. C. and Chien, K. R. (1997). Point mutations in human beta cardiac myosin heavy chain have differential effects on sarcomeric structure and assembly: an ATP binding site change disrupts both thick and thin filaments, whereas hypertrophic cardiomyopathy mutations display normal assembly. *J. Cell Biol.* **137**, 131-140.

Bonne, G., Carrier, L., Bercovici, J., Cruaud, C., Richard, P., Hainque, B., Gautel, M., Labeit, S., James, M., Beckmann, J. et al. (1995). Cardiac myosin binding protein-C gene splice acceptor site mutation is associated with familial hypertrophic cardiomyopathy. *Nature Genet.* **11**, 438-440.

Bonne, G., Carrier, L., Richard, P., Hainque, B. and Schwartz, K. (1998). Familial hypertrophic cardiomyopathy: from mutations to functional defects. *Circ. Res.* **83**, 580-593.

Bourdieu, L., Magnasco, M. O., Winkelmann, D. A. and Libchaber, A. (1995). Actin filaments on myosin beds: The velocity distribution. *Physical Review. E. Statistical Physics, Plasmas, Fluids, and Related Interdisciplinary Topics* **52**, 6573-6579.

Chow, D., Srikakulam, R., Chen, Y. and Winkelmann, D. A. (2002). Folding of the striated muscle myosin motor domain. *J. Biol. Chem.* **277**, 36799-36807.

Colognato, H., Winkelmann, D. A. and Yurchenco, P. D. (1999). Laminin polymerization induces a receptor-cytoskeleton network. *J. Cell Biol.* **145**, 619-631.

Cuda, G., Fananapazir, L., Epstein, N. D. and Sellers, J. R. (1997). The in vitro motility activity of beta-cardiac myosin depends on the nature of the beta-myosin heavy chain gene mutation in hypertrophic cardiomyopathy. *J. Muscle Res. Cell Motil.* **18**, 275-283.

Cuda, G., Fananapazir, L., Zhu, W. S., Sellers, J. R. and Epstein, N. D. (1993). Skeletal muscle expression and abnormal function of beta-myosin in hypertrophic cardiomyopathy. *J. Clin. Invest.* **91**, 2861-2865.

Eble, D. M., Qi, M., Waldschmidt, S., Lucchesi, P. A., Byron, K. L. and Samarel, A. M. (1998). Contractile activity is required for sarcomeric assembly in phenylephrine-induced cardiac myocyte hypertrophy. *Am. J. Physiol.* **274**, C1226-1237.

Fananapazir, L., Dalakas, M. C., Cyran, F., Cohn, G. and Epstein, N. D. (1993). Missense mutations in the beta-myosin heavy-chain gene cause central core disease in hypertrophic cardiomyopathy. *Proc. Natl. Acad. Sci. USA* **90**, 3993-3997.

Ferrans, V. J., Morrow, A. G. and Roberts, W. C. (1972). Myocardial ultrastructure in idiopathic hypertrophic subaortic stenosis. A study of operatively excised left ventricular outflow tract muscle in 14 patients. *Circulation* **45**, 769-792.

Franz, W. M., Muller, O. J. and Katus, H. A. (2001). Cardiomyopathies: from genetics to the prospect of treatment. *Lancet* **358**, 1627-1637.

Fujita, H., Sugiura, S., Momomura, S., Omata, M., Sugi, H. and Sutoh, K. (1997). Characterization of mutant myosins of Dictyostelium discoideum equivalent to human familial hypertrophic cardiomyopathy mutants. Molecular force level of mutant myosins may have a prognostic implication. *J. Clin. Invest.* **99**, 1010-1015.

Geisterfer-Lowrance, A. A., Kass, S., Tanigawa, G., Vosberg, H. P., McKenna, W., Seidman, C. E. and Seidman, J. G. (1990). A molecular basis for familial hypertrophic cardiomyopathy: a beta cardiac myosin heavy chain gene missense mutation. *Cell* **62**, 999-1006.

Geisterfer-Lowrance, A. A., Christe, M., Conner, D. A., Ingwall, J. S., Schoen, F. J., Seidman, C. E. and Seidman, J. G. (1996). A mouse model of familial hypertrophic cardiomyopathy. *Science* **272**, 731-734.

Hamburger, V. and Hamilton, H. L. (1992). A series of normal stages in the development of the chick embryo. 1951. *Dev. Dyn.* **195**, 231-272.

Harada, Y., Sakurada, K., Aoki, T., Thomas, D. D. and Yanagida, T. (1990). Mechanochemical coupling in actomyosin energy transduction studied by in vitro movement assay. *J. Mol. Biol.* **216**, 49-68.

He, T. C., Zhou, S., da Costa, L. T., Yu, J., Kinzler, K. W. and Vogelstein, B. (1998). A simplified system for generating recombinant adenoviruses. *Proc. Natl. Acad. Sci. USA* **95**, 2509-2514.

Kim, S. J., Iizuka, K., Kelly, R. A., Geng, Y. J., Bishop, S. P., Yang, G., Kudej, A., McConnell, B. K., Seidman, C. E., Seidman, J. G. et al. (1999). An alpha-cardiac myosin heavy chain gene mutation impairs contraction and relaxation function of cardiac myocytes. *Am. J. Physiol.* **276**, H1780-H1787.

Kimura, A., Harada, H., Park, J. E., Nishi, H., Satoh, M., Takahashi, M., Hiroi, S., Sasaoka, T., Ohbuchi, N., Nakamura, T. et al. (1997). Mutations in the cardiac troponin I gene associated with hypertrophic cardiomyopathy. *Nat. Genet.* **16**, 379-382.

Kinose, F., Wang, S. X., Kidambi, U. S., Moncman, C. L. and Winkelmann, D. A. (1996). Glycine 699 is pivotal for the motor activity of skeletal muscle myosin. *J. Cell Biol.* **134**, 895-909.

Ko, Y. L., Chen, J. J., Tang, T. K., Cheng, J. J., Lin, S. Y., Liou, Y. C., Kuan, P., Wu, C. W., Lien, W. P. and Liew, C. C. (1996). Malignant familial hypertrophic cardiomyopathy in a family with a 453Arg→Cys mutation in the beta-myosin heavy chain gene: coexistence of sudden death and end-stage heart failure. *Hum. Genet.* **97**, 585-590.

Kropp, K. E., Gulick, J. and Robbins, J. (1987). Structural and transcriptional analysis of a chicken myosin heavy chain gene subset. *J. Biol. Chem.* **262**, 16536-16545.

Laing, N. G., Wilton, S. D., Akkari, P. A., Dorosz, S., Boundy, K., Kneebone, C., Blumbergs, P., White, S., Watkins, H., Love, D. R. et al. (1995). A mutation in the alpha tropomyosin gene TPM3 associated with autosomal dominant nemaline myopathy [published erratum appears in Nat. Genet. 1995 Jun;10(2):249] [see comments]. *Nature Genet.* **9**, 75-79.

Lankford, E. B., Epstein, N. D., Fananapazir, L. and Sweeney, H. L. (1995). Abnormal contractile properties of muscle fibers expressing beta-myosin heavy chain gene mutations in patients with hypertrophic cardiomyopathy. *J. Clin. Invest.* **95**, 1409-1414.

Maass, A. and Leinwand, L. A. (2000). Animal models of hypertrophic cardiomyopathy. *Curr. Opin. Cardiol.* **15**, 189-196.

Marian, A. J., Wu, Y., Lim, D. S., McCluggage, M., Youker, K., Yu, Q. T., Brugada, R., DeMayo, F., Quinones, M. and Roberts, R. (1999). A transgenic rabbit model for human hypertrophic cardiomyopathy. *J. Clin. Invest.* **104**, 1683-1692.

Miller, G., Colegrave, M. and Peckham, M. (2000). N232S, G741R and D778G beta-cardiac myosin mutants, implicated in familial hypertrophic cardiomyopathy, do not disrupt myofibrillar organisation in cultured myotubes. *FEBS Lett.* **486**, 325-327.

Miller, G., Maycock, J., White, E., Peckham, M. and Calaghan, S. (2003). Heterologous expression of wild-type and mutant {beta}-cardiac myosin changes the contractile kinetics of cultured mouse myotubes. *J. Physiol.* **548**, 167-174.

Miller, J. B., Teal, S. B. and Stockdale, F. E. (1989). Evolutionarily conserved sequences of striated muscle myosin heavy chain isoforms. Epitope mapping by cDNA expression. *J. Biol. Chem.* **264**, 13122-13130.

Mogensen, J., Klausen, I. C., Pedersen, A. K., Egeblad, H., Bross, P., Kruse, T. A., Gregersen, N., Hansen, P. S., Baandrup, U. and Borglum, A. D. (1999). Alpha-cardiac actin is a novel disease gene in familial hypertrophic cardiomyopathy. *J. Clin. Invest.* **103**, R39-43.

Molina, M. I., Kropp, K. E., Gulick, J. and Robbins, J. (1987). The sequence of an embryonic myosin heavy chain gene and isolation of its corresponding cDNA. *J. Biol. Chem.* **262**, 6478-6488.

Moncman, C. L. and Wang, K. (1995). Nebulette: a 107 kD nebulin-like protein in cardiac muscle. *Cell Motil. Cytoskeleton* **32**, 205-225.

Moncman, C. L. and Wang, K. (1996). Assembly of nebulin into the sarcomeres of avian skeletal muscle. *Cell Motil. Cytoskeleton* **34**, 167-184.

Moncman, C. L. and Wang, K. (2002). Targeted disruption of nebulette protein expression alters cardiac myofibril assembly and function. *Exp. Cell. Res.* **273**, 204-218.

Moncman, C. L., Rindt, H., Robbins, J. and Winkelmann, D. A. (1993). Segregated assembly of muscle myosin expressed in nonmuscle cells. *Mol. Biol. Cell* **4**, 1051-1067.

Moss, R. L. and Periera, J. S. (2000). Enhanced myosin function due to a point mutation causing a familial hypertrophic cardiomyopathy. *Circ. Res.* **86**, 720-722.

Palmiter, K. A., Tyska, M. J., Haeberle, J. R., Alpert, N. R., Fananapazir, L. and Warshaw, D. M. (2000). R403Q and L908V mutant beta-cardiac myosin from patients with familial hypertrophic cardiomyopathy exhibit enhanced mechanical performance at the single molecule level. *J. Muscle Res. Cell Motil.* **21**, 609-620.

Poetter, K., Jiang, H., Hassanzadeh, S., Master, S. R., Chang, A., Dalakas, M. C., Rayment, I., Sellers, J. R., Fananapazir, L. and Epstein, N. D. (1996). Mutations in either the essential or regulatory light chains of myosin are associated with a rare myopathy in human heart and skeletal muscle. *Nat. Genet.* **13**, 63-69.

Rabkin, S. W. (1993). Comparison of indapamide and hydrochlorothiazide on spontaneous contraction of cardiomyocytes in culture: the effect on alterations of extracellular calcium or potassium. *Gen. Pharmacol.* **24**, 699-704.

Ramachandran, I., Terry, M. and Ferrari, M. B. (2003). Skeletal muscle myosin cross-bridge cycling is necessary for myofibrillogenesis. *Cell Motil. Cytoskeleton* **55**, 61-72.

Rayment, I., Rypniewski, W. R., Schmidt-Base, K., Smith, R., Tomchick, D. R., Benning, M. M., Winkelmann, D. A., Wesenberg, G. and Holden, H. M. (1993). Three-dimensional structure of myosin subfragment-1: a molecular motor. *Science* **261**, 50-58.

Rayment, I., Holden, H. M., Sellers, J. R., Fananapazir, L. and Epstein, N. D. (1995). Structural interpretation of the mutations in the beta-cardiac myosin that have been implicated in familial hypertrophic cardiomyopathy. *Proc. Natl. Acad. Sci. USA* **92**, 3864-3868.

Seidman, C. E. and Seidman, J. G. (2000). Hypertrophic Cardiomyopathy. In *The Metabolic and Molecular Bases of Inherited Disease* (ed. C. R. Scriver, A. L. Beaudet, D. Valle, W. S. Sly, B. Childs, K. W. Kinzler and B. Vogelstein), pp. 5433-5452. New York, NY: McGraw-Hill.

Seidman, J. G. and Seidman, C. (2001). The genetic basis for cardiomyopathy: from mutation identification to mechanistic paradigms. *Cell* **104**, 557-567.

Siemering, K. R., Golbik, R., Sever, R. and Haseloff, J. (1996). Mutations that suppress the thermosensitivity of green fluorescent protein. *Curr. Biol.* **6**, 1653-1663.

Soeno, Y., Shimada, Y. and Obinata, T. (1999). BDM (2,3-butanedione monoxime), an inhibitor of myosin-actin interaction, suppresses myofibrillogenesis in skeletal muscle cells in culture. *Cell Tissue Res.* **295**, 307-316.

Sweeney, H. L., Straceski, A. J., Leinwand, L. A., Tikunov, B. A. and Faust, L. (1994). Heterologous expression of a cardiomyopathic myosin that is defective in its actin interaction. *J. Biol. Chem.* **269**, 1603-1605.

Thierfelder, L., Watkins, H., MacRae, C., Lamas, R., McKenna, W., Vosberg, H. P., Seidman, J. G. and Seidman, C. E. (1994). Alpha-tropomyosin and cardiac troponin T mutations cause familial hypertrophic cardiomyopathy: a disease of the sarcomere. *Cell* **77**, 701-712.

Towbin, J. A. (2001). Molecular genetic basis of sudden cardiac death. *Cardiovasc. Pathol.* **10**, 283-295.

Tyska, M. J., Hayes, E., Giewat, M., Seidman, C. E., Seidman, J. G. and Warshaw, D. M. (2000). Single-molecule mechanics of R403Q cardiac myosin isolated from the mouse model of familial hypertrophic cardiomyopathy. *Circ. Res.* **86**, 737-744.

Uyeda, T. Q., Kron, S. J. and Spudich, J. A. (1990). Myosin step size. Estimation from slow sliding movement of actin over low densities of heavy meromyosin. *J. Mol. Biol.* **214**, 699-710.

Viatchenko-Karpinski, S., Fleischmann, B. K., Liu, Q., Sauer, H., Gryshchenko, O., Ji, G. J. and Hescheler, J. (1999). Intracellular Ca2+ oscillations drive spontaneous contractions in cardiomyocytes during early development. *Proc. Natl. Acad. Sci. USA* **96**, 8259-8264.

Watkins, H., Rosenzweig, A., Hwang, D. S., Levi, T., McKenna, W., Seidman, C. E. and Seidman, J. G. (1992). Characteristics and prognostic implications of myosin missense mutations in familial hypertrophic cardiomyopathy [see comments]. *New Eng. J. Med* **326**, 1108-1114.

Watkins, H., Conner, D., Thierfelder, L., Jarcho, J. A., MacRae, C., McKenna, W. J., Maron, B. J., Seidman, J. G. and Seidman, C. E. (1995a). Mutations in the cardiac myosin binding protein-C gene on chromosome 11 cause familial hypertrophic cardiomyopathy. *Nat. Genet.* **11**, 434-437.

Watkins, H., McKenna, W. J., Thierfelder, L., Suk, H. J., Anan, R., O'Donoghue, A., Spirito, P., Matsumori, A., Moravec, C. S., Seidman, J. G. et al. (1995b). Mutations in the genes for cardiac troponin T and alpha-tropomyosin in hypertrophic cardiomyopathy. *New Eng. J. Med.* **332**, 1058-1064.

Watkins, H., Seidman, J. G. and Seidman, C. E. (1995c). Familial hypertrophic cardiomyopathy: a genetic model of cardiac hypertrophy. *Hum. Mol. Genet.* **4**, 1721-1727.

Winkelmann, D. A., Kinose, F. and Chung, A. L. (1993). Inhibition of actin filament movement by monoclonal antibodies against the motor domain of myosin. *Journal of Muscle Res. Cell Motil.* **14**, 452-467.

Winkelmann, D. A., Bourdieu, L., Ott, A., Kinose, F. and Libchaber, A. (1995). Flexibility of myosin attachment to surfaces influences F-actin motion. *Biophy. J.* **68**, 2444-2453.

Yamashita, H., Tyska, M. J., Warshaw, D. M., Lowey, S. and Trybus, K. M. (2000). Functional consequences of mutations in the smooth muscle myosin heavy chain at sites implicated in familial hypertrophic cardiomyopathy. *J. Biol. Chem.* **275**, 28045-28052.

Yang, F., Moss, L. G. and Phillips, G. N., Jr (1996). The molecular structure of green fluorescent protein. *Nat. Biotechnol.* **14**, 1246-1251.